Wärme- und Stoffübertragung 14, 231-244 (1980)

Wärme- und Stoffübertragung
Thermo- and Fluid Dynamics



# Unsteady Heat Transfer with Solidification Applied to the Fluidity of Pure Metals*

M. Kölling and U. Grigull, München

Abstract. The entrance flow of molten metals into horizontal cylinders until their solidification has been studied. A mathematical model describes temperature field and mean velocities in that part of the cylinder just filled at each time. Thus fluidity as maximum flow length can be calculated as a function of known properties only. An empirical heat transfer coefficient is avoided by postulating a concentric air-gap which is formed by thermal contraction of the solidified annulus. - Casting experiments with pure metals such as Sn, Pb, Zn, and Al have been conducted for different temperatures and metal-heads. The flow function was measured with small photo-cells in a cylindrical metal form (Ø 5 mm). The dependence of fluidity from material properties and casting parameters is predicted by a general formula, derived from the numerical results, and is verified also by similar experiments by other authors.

Instationäre Wärmeübertragung mit Erstarrung am Beispiel des Fließvermögens reiner Metalle

Zusammenfassung. Der Einströmvorgang metallischer Schmelzen in horizontale Zylinder wurde bis zu ihrer Erstarrung untersucht. Ein mathematisches Modell beschreibt das Temperaturfeld und die mittleren Geschwindigkeiten in dem Teil des Zylinders, der zu jedem Zeitpunkt gerade gefüllt ist. Damit kann das Fließvermögen als maximale Fließlänge allein aufgrund bekannter Größen berechnet werden. Ein empirischer Wärmeübergangskoeffizient wird nämlich dadurch umgangen, daß ein konzentrischer Luftspalt postuliert wird, der sich durch die Schrumpfung des erstarrten Metallringes bildet. - Gießversuche wurden mit reinen Metallen wie Sn, Pb, Zn und Al bei unterschiedlichen Gießtemperaturen und Druckhöhen durchgeführt. Die Fließfunktion wurde dabei mit kleinen Lichtschranken im zylindrischen Metallkanal (Ø 5 mm) gemessen. Die Abhängigkeit wird von einer allgemeinen Gleichung vorausgesagt, die aus den numerischen Ergebnissen abgeleitet wurde, und auch von ähnlichen Messungen anderer Autoren bestätigt.

## Nomenclature

| | |
|---|---|
| $a$ | thermal diffusivity |
| $c$ | specific heat at constant pressure |
| DR | radial mesh point distance, $\Delta r/R_0$ |
| DX | axial distance of mesh points, $\Delta x/R_0$ |
| DFo | dimensionless timestep, $\Delta t \cdot a/R_0^2$ |
| Fo | Fourier number, $a \cdot t/R_0^2$ |
| $g$ | acceleration of gravity |
| $h_s$ | specific heat of fusion (latent heat) |
| $H$ | geodatic height (metal head) |
| $i$ | radial numbering index |
| $j$ | axial numbering index |
| $k$ | numbering index for time steps |
| $L$ | maximum flow length (fluidity) |
| $m$ | number of radial meshlines |
| $m_w$ | number of meshlines in the channel interior |
| $n$ | number of meshrows |
| Ph | phasechange number, $h_s/c_s/(\vartheta_s - \vartheta_u)$ |
| Pr | Prandtl number, $\nu/a_1$ |
| $r$ | radial coordinate |
| $R$ | radius of flow cross section |
| Re | Reynolds number, $u \cdot R_0/\nu$ |
| $t$ | time coordinate |
| $T$ | dimensionless temperature, $(\vartheta - \vartheta_u)/(\vartheta_s - \vartheta_u)$ |
| $u$ | axial velocity |
| $w$ | wall thickness |
| $x$ | axial coordinate |

## Greek Symbols

| | |
|---|---|
| $\alpha$ | constant |
| $\beta$ | coefficient of linear expansion |
| $\delta$ | thickness of solidified annulus + airgap |
| $\delta_a$ | thickness of airgap |
| $\Delta$ | difference |
| $\vartheta$ | temperature |
| $\vartheta_s$ | solidification temperature |
| $\vartheta_u$ | ambient (wall) temperature |
| $\lambda$ | thermal conductivity |
| $\nu$ | kinematic viscosity |
| $\rho$ | density |
| $\tau$ | solidification time |
| $\Phi$ | heat source at the phase boundary |

* Extract of the Doctoral Thesis "Instationäre Wärmeübertragung mit Erstarrung am Beispiel des Fließvermögens reiner Metalle" from Dipl.-Ing. M. Kölling, Fachbereich Maschinenwesen, Technische Universität München, W.-Germany, 1980

0042-9929/80/0014/0231/$ 2.80

Superscripts

| | |
|---|---|
| * | values (coordinates) divided by $R_0$ |
| – | average value |
| a | refers to air |
| l | refers to liquid phase |
| m | mean values |
| o | refers to flow front, initial values |
| p | refers to moving phase boundary |
| s | refers to solid phase |
| w | refers to wall |

## 1 Introduction

Heat transfer problems with phase change liquid/solid have been subject to many papers since the end of the last century. J. Stefan [27] and F. Neumann were the first to study heat conduction analytically during melting or solidification. Since then this problem, usually referred to as Stefan-problem, with its non-linearity at the moving boundary has been generalized to more complicated boundary conditions and multidimensional cases. A good literature review till about 1964 is given by Muehlbauer & Sunderland [18] who subdivide the papers according to the different approach of solution. But all these papers, to which the work of Goodrich [8] and that of Sparrow et al. [26] may be added as more recent contributions to that topic, are concerned with heat conduction only. There are very few publications which consider solidification in flow problems.

The quasi-stationary flow problem seems to be theoretically studied by Beaubouef & Chapman [1] first and then advanced to more general cases by Stephan [28], Siegel & Savino [23], Genthner [7]. An experimental investigation of unsteady pipe flow with solidification of saturated water, benzene and freon 112 A has been reported by Epstein et al. [4]. A similar problem with molten metals shall be subject of this paper.

Foundrymen are often interested to know how easily a molten metal may fill the mold. To characterize the castability of a metal or alloy they measure its fluidity which is defined as the maximum flow length that the molten metal can flow in a special test form under certain applied casting conditions before it completely solidifies at a specific position in the mold.

There are many different test forms with different cross sections for the horizontal channel, with different materials and different casting - as well as gating systems. Thus the test results are hardly comparable; but for a special application in most cases just the qualitative influence of casting temperature, metal head and mold temperature on the fluidity of a metal is of interest. Attempts to generally describe this complex quantity, involving more than just material properties of the metal, have not really been successful since an empirical constant is always still needed (Ragone et al. [20]).

This paper is concerned with the quantitative description of fluidity as a sole function of material properties and known initial- and boundary conditions for temperature and velocity. This is tried by modelling the phenomenon as a pipe flow problem with internal solidification. Of course, the real situation in the channel must be somewhat simplified. Thus, in a first step, the analysis has been restricted to pure metals since they solidify with a rather smooth interface at a distinct temperature. The model predictions are verified by casting experiments with some pure low melting metals in a straight cylindrical channel form (Ø 5 mm) of a Ni-Cr alloy (Inconel 600). Fluidity and flow function are measured for different casting temperatures and metal heads. The results are also compared with those from literature.

## 2 Mathematical Model of Fluidity

### 2.1 Simplifying Assumptions

To set up a model of fluidity one first has to discuss the assumptions, which simplify the real physical problem associated with fluidity, in order to avoid an undue mathematical effort. First of all it shall be assumed that for the cylindrical problem only two dimensions are of importance. Thus effects of gravity are neglected in the horizontal channel. Secondly it is assumed that the circled quantities (initial- and boundary conditions) in Fig. 1 are known, which shows the situation in the filled section of the channel at a time $t > 0$. This means the exclusion of any strange effects which may occur by manual casting

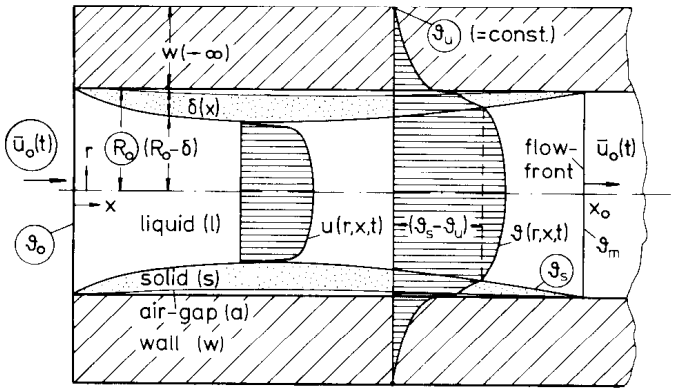


Fig. 1. Conception of the physical problem with symbols and initial- and boundary values as circled quantities

through different casting systems with gating. It implies also the experience that for practical molds the wall is thick enough so that during the interesting time period the outer surface will remain isothermal ($\vartheta_u$ = const.). The molten metal shall uniformly flow into the empty channel with a plane flow-front and a mean velocity $\bar{u}_0$ according to a constant metal head H. As soon as the melt cools down below its solidification temperature it shall isotropicly solidify with a smooth interface without supercooling. This assumtion is in rather good agreement with the behavior of pure metals (Flemings [6]) to which this model is therefore limited. The liberated latent heat at the phase boundary shall be considered by a moving line source. A rather crude simplification is the assumption of a quasi-stationary, turbulent bulb flow for the liquid flow. But since the knowledge of such flows is not very reliable a more sophisticated description does not seem to be worth the effort. Therefore the pressure drop in the channel, regarding its diminishing cross section R because of the solidified annulus (Fig. 1), is determined by a friction factor for fully developed pipe flow according to the Blasius formula. The velocity distribution shown in Fig. 1 corresponds to the 1/7 power law suitable for turbulent flows which is assumed for the formulation of the heat convection terms because it is numerically easier to handle than the step-function of a bulb-profile. It is known that the heat transfer between metal and wall is not ideal, i.e. the two phases are not in direct thermal contact. But instead of introducing an empirical heat transfer coefficient as usual a concentric air-gap is postulated which is formed by thermal contraction of the solidified annulus. This situation is illustrated also by the qualitative temperature distribution in Fig. 1. The boundary condition at the moving flow front $x_0$ is assumed to be adiabatic for the sake of simplicity and numerical advantage. According to the conception of turbulent mixing the temperature $\vartheta_m$ can easily be calculated as new initial value at any time at the flow-front. Furthermore constant properties are assumed to describe the different phases, which seems reasonable regarding the moderate temperature dependence of most of the thermal properties [25, 29, 30]. And finally surface forces shall be negligible as compared to pressure forces applied by the metal head.

## 2.2 Governing Equations

With the above mentioned assumptions one now can derive the equations governing the problem from the general conservation laws for energy, momentum and mass. It shall be done in dimensionless form with the definition of the variables according to the nomenclature.

$$\frac{\partial T}{\partial Fo} = \frac{\partial^2 T}{\partial r^{*2}} + \frac{\partial^2 T}{\partial x^{*2}} + \frac{1}{r^*} \cdot \frac{\partial T}{\partial r^*} - Pr \cdot Re \cdot \frac{\partial T}{\partial x^*} + \Phi \,. \tag{1}$$

Equation (1) is the unsteady, two-dimensional energy equation in cylindrical coordinates with the last two terms representing heat convection and heat source at the moving phase boundary respectively. This equation describes the temperature field in the whole section of the channel just filled at each time. The different phases are considered by space dependent properties with special conditions at the interfaces, which will be discussed later on.

According to the assumptions concerning the melt flow in the channel the general equation of motion (Bird et al. [2]) can be written as follows:

$$\overline{Re}(0)^2 = \overline{Re}_0^2 + \int_0^{x_0^*} \frac{0.3164 \cdot \overline{Re}^2}{[2 \cdot (1 - \delta^*) \cdot \overline{Re}]^{1/4}} \cdot \frac{dx}{2 \cdot (1 - \delta^*)} \,. \tag{2}$$

It is the determining equation for the mean velocity $\overline{Re}_0$ of the flow-front with its initial value $\overline{Re}(0)$

and the Blasius formula for the friction factor. This equation is coupled with the energy Eq.(1) through the dimensionless thickness $\delta^*$ of the solidified annulus. This quantity also gives us the relation between $\overline{Re}_0$ and the mean velocity $\overline{Re}$ at any position $x^*$ along the channel necessary to solve the integral of Eq.(2). It is just the special formulation of the continuity equation, neglecting the influence of density differences:

$$\overline{Re}_0 = \overline{Re} \cdot (1 - \delta^*)^2 \ . \qquad (3)$$

In addition to these fundamental equations we still have to specify the local distribution of Re and $\Phi$ in Eq.(1). The velocity is defined in the liquid region according to the 1/7 power law and vanishes every where else:

$$Re = \begin{cases} 1.22 \cdot \overline{Re} \cdot \left(1 - \frac{r^*}{1 - \delta^*}\right)^{1/7} & \text{for } 0 \leqslant r^* \leqslant (1 - \delta^*) \\ 0 & \text{for } r^* > (1 - \delta^*) \end{cases} . \qquad (4)$$

The heat source $\Phi$ only exists at the moving phase boundary and is proportional to its velocity and the specific heat of fusion:

$$\Phi = \begin{cases} 0 & \text{for } r^* \neq (1 - \delta^*) \\ Ph \cdot \frac{\partial}{\partial Fo_m} \left(\frac{d\delta^*}{dr^*}\right) & \text{for } r^* = (1 - \delta^*) \end{cases} . \qquad (5)$$

The quotient $(d\delta^*/dr^*)$ in Eq.(5) is just a ratio of liquid to solid volume resulting from a radial energy balance on a stationary element at the interface. To complete the system of equations the initial- and boundary conditions as well as the coupling conditions at the interfaces of the different phases are to be stated. At time Fo = 0 the molten metal with its casting temperature $T_0$ starts to enter the empty channel. Therefore the flow-front $x_0^*$ is at the channel entrance, and the initial conditions for temperature and mean velocity (for local velocity see Eq.(4)) are as follows:

$$Fo = 0: \quad x_0^* = 0; \quad \delta^* = 0; \quad \delta_a^* = 0$$

$$T = \begin{cases} T_0 & \text{for } 0 \leqslant r^* < 1 \\ 0 & \text{for } r^* \geqslant 1 \end{cases}$$

$$\overline{Re}_0 = \overline{Re}(0) \ . \qquad (6)$$

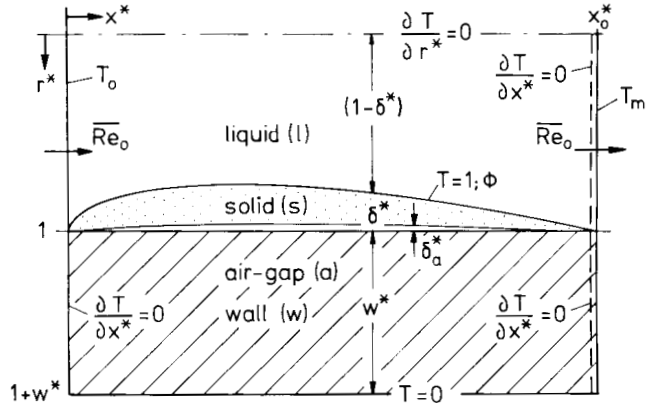


Fig.2. Boundary conditions for governing equations of the mathematical model considering only one half of the symmetric channel at Fo > 0 ($x_0^* > 0$)

Since the length $x_0^*$ of the problem varies with time according to the mean flow-front velocity the newly created region $dx_0^*$ requires initial values for temperature for each time step. A mixing temperature $T_m$ is assumed in the liquid phase, and in the wall phase somewhat arbitrarily the neighboring temperature $T_{x_0^*}$ is assumed:

$$T_{x_0^*+dx_0^*} = \begin{cases} \int_0^1 T_{x_0^*} \cdot Re \cdot r^* \cdot dr^* \Big/ \int_0^1 Re \cdot r^* \cdot dr^* & \text{for } 0 \leqslant r^* < 1 \\ T_{x_0^*} & \text{for } r^* \geqslant 1 \end{cases} \qquad (7)$$

The boundary conditions are collected in the sketch of Fig.2 which shows one half of the symmetric problem.

It also contains the conditions at the interfaces of the different phases. These coupling conditions are the assumptions that the phase change boundary is identical with the solidification isotherm

$$T(r^* = 1 - \delta^*) = 1 \ , \qquad (8)$$

and that the heat transfer at the inner wall surface is described by the heat conduction through an air-gap. The thickness of this air-gap is determined by the thermal contraction of the solidified annulus, thus by the coefficient of linear expansion $\beta$ and the temperature difference between the actual surface temperature of the annulus and its solidification temperature, as it is explained by Fig.3.

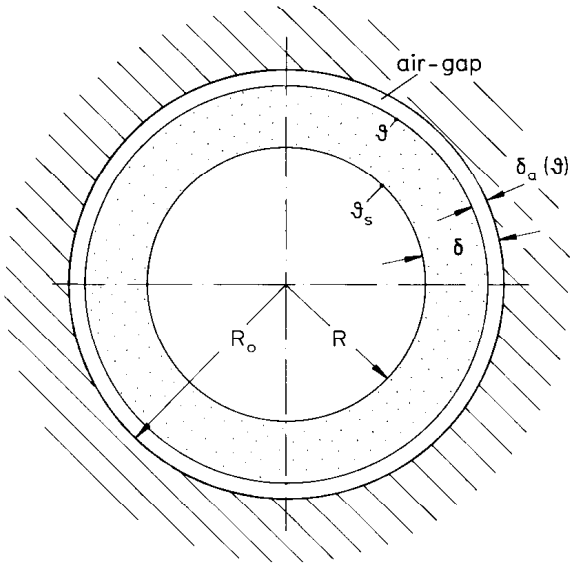


Fig. 3. Channel cross section with solidified annulus and concentric air-gap

$$\delta_a^* = \beta \cdot (\vartheta_s - \vartheta_u) \cdot [1 - T(r^* = 1 - \delta_a^*)] \quad \text{for} \quad \delta^* > 0 \ . \tag{9}$$

Of course, the solidified annulus first must have a finite thickness before it can shrink against the liquid pressure. But this will be automatically considered through the numerical solution procedure where the surface temperature will actually be represented by the discrete temperature of a finite volume element, which will be discussed in more detail in the next chapter.

## 2.3 Numerical Solution Procedure

For the solution of the system of equations governing the mathematical model there is no direct analytical method known yet. Therefore a numerical solution approach has been chosen here, more specifically the finite difference method (FDM) for the differential equation (1) and the trapezoid rule for the integral of Eq. (2).

Together with the pure implicit approximation for evaluating the time differential the FDM is unconditionally stable and relatively easy to handle, which is rather important for the variable length in axial direction of this problem. It also has been verified rather extensively by now so that good literature can be found on this technique [16, 19, 22, 24]. Thus the solution procedure shall only be discussed as detailed as it is needed for good unterstanding.

In differencing techniques the region under consideration always has to be subdivided into a finite number of discrete elements (mesh). The channel here is discretized by annular elements with the constant dimensions DR in radial and DX in axial direction. This is done in a way that the central elements (i = 1) surround the centre line and the inner wall surface coincides with an element boundary ($i = m_w$). The area centre (mesh point) of the last element in radial direction (i = m + 1) shall lie on the outer wall surface which is according to the assumptions (Fig. 2) isothermal with the known temperature T = 0. Then the mesh point distance DR is determined either by the number m or $m_w$:

$$DR = \frac{1 + w^*}{m} = \frac{1}{m_w - 0.5} \ . \tag{10}$$

The axial distance DX influences the length of each timestep because the boundary of the last mesh element (j = n) follows the flow-front stepwise, with n being variable and equal to the number of timesteps (n = k). Therefore it should not be too small (economy), numerical accuracy, however, recommends the value of DR not to be exceeded three times:

$$DX \leqslant 3 \cdot DR \ . \tag{11}$$

Having chosen the two dimensions of the mesh elements the timestep is also determined through the link of flow front velocity and mesh point distance DX:

$$DFo_{1(a=a_1)} = \frac{1}{Pr} \cdot \frac{DX}{\overline{Re}_0} \ . \tag{12}$$

The index 1 of DFo indicates that the timestep $\Delta t$ is here formed dimensionless by the thermal diffusivity of the liquid metal phase through the Pr-number.

With these difference parameters the differential energy equation can be formulated for each mesh point in difference form assuming linear variation of temperature between those points. This is done in the same way as described in literature. The special condition at the centre line of the cylindrical problem is considered by the well-known MacLaurin approximation (Smith [24]). The first order differentials are

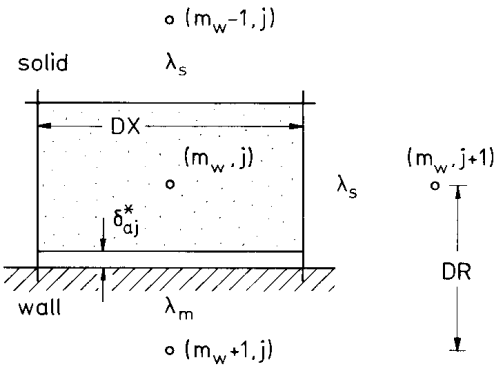


Fig. 4. Mesh element at the interface of the inner wall surface with air-gap

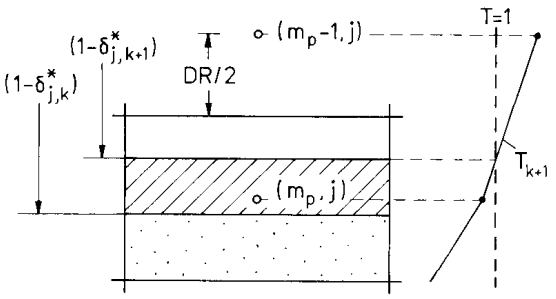


Fig. 5. Movement of the phase boundary (T = 1) during one timestep $DFo_{k+1}$

approximated by a pure implicit method for the time derivative, a central difference for the radial differential and a sort of upwind difference for the convection term which proved to be most suitable for this kind of problem:

$$Pr \cdot Re \cdot \frac{\partial T}{\partial x^*} \approx Pr \cdot Re_{i,j} \cdot \frac{T_{i,j} - T_{i,j-1}}{DX} \quad . \qquad (13)$$

The boundary conditions (Fig. 2) are not difficult to consider, but it has yet to be explained how the coupling conditions on the interfaces of the different phases shall be handled. Let us first look at the situation at the inner wall surface as it is demonstrated by Fig. 4. The mesh element $(m_w, j)$ shall have already been solidified so that an air-gap, being always smaller than DR/2 by choice of DR, is attributed to the solidified element so that its heat capacity has to be altered. Neglecting the capacity of air and the curvature of the annular air-gap this can be done in the following way:

$$(\rho \cdot c)_m \approx (1 - \delta^*_{aj}/DR) \cdot \rho_s \cdot c_s \quad . \qquad (14)$$

The thermal link of the mesh points $(m_w, j)$ and $(m_w + 1, j)$ across the air-gap is approximated by a mean conductivity $\lambda_m$, calculated according to the thermal resistance of a composite wall (Grigull and Sandner [9]), again neglecting the curvature of the cylindrical geometry:

$$\frac{1}{\lambda_m} \approx \frac{0.5 - \delta^*_{aj}/DR}{\lambda_s} + \frac{\delta^*_{aj}/DR}{\lambda_a} + \frac{0.5}{\lambda_w} \quad . \qquad (15)$$

If the air-gap does not yet exist only two phases are to be considered, which of course is even less difficult. A similar situation is given at the other interface, the moving phase boundary, where the coupling condition is handled in an equivalent way. But in addition to the unsteady change of properties (also averaged by mean values - Index m) at that interface, usually not coincident with an element boundary, the latent heat is liberated there. This heat source is uniformly smeared over the area which the phase boundary passes over during one time step. This area is indicated in Fig. 5 by parallel lines; there it only covers part of the element $(m_p, j)$ so that the heat source solely appears in the difference equation for the temperature $T_{m_p,j,k+1}$ and is considered as follows (see also equation (5)):

$$DFo_m \cdot \Phi_j = Ph \cdot \frac{\rho_s \cdot c_s}{(\rho \cdot c)_m} \cdot \Delta\delta^*_j / DR \quad . \qquad (16)$$

Since the problem is cylindrical one might correct the space difference $\Delta\delta^*_j$, being sufficiently accurate only for $m_p > m_w/2$, by a volume ratio:

$$\Delta\delta^*_j = (\delta^*_{j,k+1} - \delta^*_{j,k}) \cdot \begin{cases} (1 - \delta^*_{j,k+1})/(m_p - 1)/DR \\ \qquad\qquad \text{for } m_p > 1 \\ (1 - \delta^*_{j,k+1}) \cdot 4/DR \text{ for } m_p = 1 \, . \end{cases} \qquad (17)$$

Up to now we have discussed how to obtain $m \times n$ linear equations from the energy equation (1) by means of the pure implicit finite difference method. These equations can be solved by a modified Gauss algorithm. From the resulting temperature field we get the solidification isotherm by interpolation be-

tween the respective temperatures (Fig.5). This serves to control the position of the liquid/solid interface which has to be estimated first to evaluate the velocities and the heat source (Eqs.(2), (4) and (16)). When the estimation and the calculated values have sufficiently approached the iteration has succeeded and the next time-step can be calculated. It starts with extension of the mesh by one row (n + 1) and specification of the initial values there (Eq.(7)). Again the new thickness of the solidifying annulus and also of the air-gap must be estimated and then successively improved by iteration. This solution procedure is followed in the same way for each timestep till the solidification front reaches the centre line and thereby blocks off the metal flow.

The fluidity is then proportional to the number of mesh rows n and is determined by equation (18):

$$L = n \cdot DX \cdot R_0 \quad . \tag{18}$$

Since the solution has been obtained numerically one has to look for the calculation errors; in this case, however, the question is very difficult to answer. There is no exact solution for comparison, and the Neumann solution for the simple one-dimensional Stefan-problem only can serve as a check on computational correctness and can give an estimate on the mesh point number needed for a desired accuracy. The other way of varying the discretization parameters as long as the results do not change any more is also limited because of the computer storage available (CDC, Cyber 175 × 2). The error, of course, does not depend only on mesh spacing but also on property values, but estimations suggest that for usual conditions with m = 16 ($m_w$ = 10) and DX = 0,25 the numerical error should not exceed 5% (see Kölling [12]).

Even more than numerical accuracy it seems to be important that the model predictions prove true compared with reality. Therefore experiments have been conducted especially considering the assumptions concerning the initial- and boundary conditions in the mathematical model.

## 3 Experimental Verification

### 3.1 Set-up for Casting Experiments

For the measurement of fluidity there have been many different forms to simulate the actual mold. The straight channel form considered here has been used eg by Klein and Fischer [11], Lang [15], Morita [17], (for further reference see [14]). They all built it from metal rather than sand but with different cross sections. To verify the theoretical results here a circular cylinder was chosen milled into two halfs of a NiCr-alloy (Inconel 600, [10]). The metal bars are fitted together by conical bolts and fixed by clamping jaws (Fig.6). The outer cross section of the form of 60 × 60 mm means a wall thickness of more than 25 mm for the Ø 5 mm channel pipe and thus ensures the validity of the assumption concerning the isothermal condition on the outer channel surface. The channel is 800 mm long enough for superheating degrees of $T_0$ = 1.8 and metal heads up to H = 200 mm. The melt is fed into the horizontal channel through a casting system connected to the channel by four screws. It is also divisible for unmolding the solidified cast piece and made of an asbestos-ceramics compound (Molten Metal Marinite) which usually is used for insulating furnaces and is very easily machinable. Its task is to change direction of the melt flow and to provide an uniform feed at constant temperature and pressure. Different shapes of the deflection system, however, could not meet the first demand sufficiently, so that a styropor bulb was introduced to avoid droplets preceding the uniform inlet flow. Thus the styropor acts as a buffer which then evaporizes very quickly at temperatures above 200 °C. It works satisfactorily for bulb-lengths of 3 to 4 mm when the bulb is slightly pressed into the horizontal flow part of the casting system.

Pure metals are filled into the crucible before it is put into the oven for melting (temperature controlled up to 1000 °C). For Sn and Pb the crucible is machined out of stainless steel as schematically shown in Fig.6. It has a plug which can be drawn for pouring the melt into the casting system. A cover prevents considerable heat losses during transportation from melting oven to casting system. The bottom shape is designed to realize quick and uniform pouring. - The dissolving behavior of Zn and especially Al to almost all metal materials forbids the use of the described crucible; therefore these metals are manually poured into the casting system with commercial crucibles of ceramics or graphite.

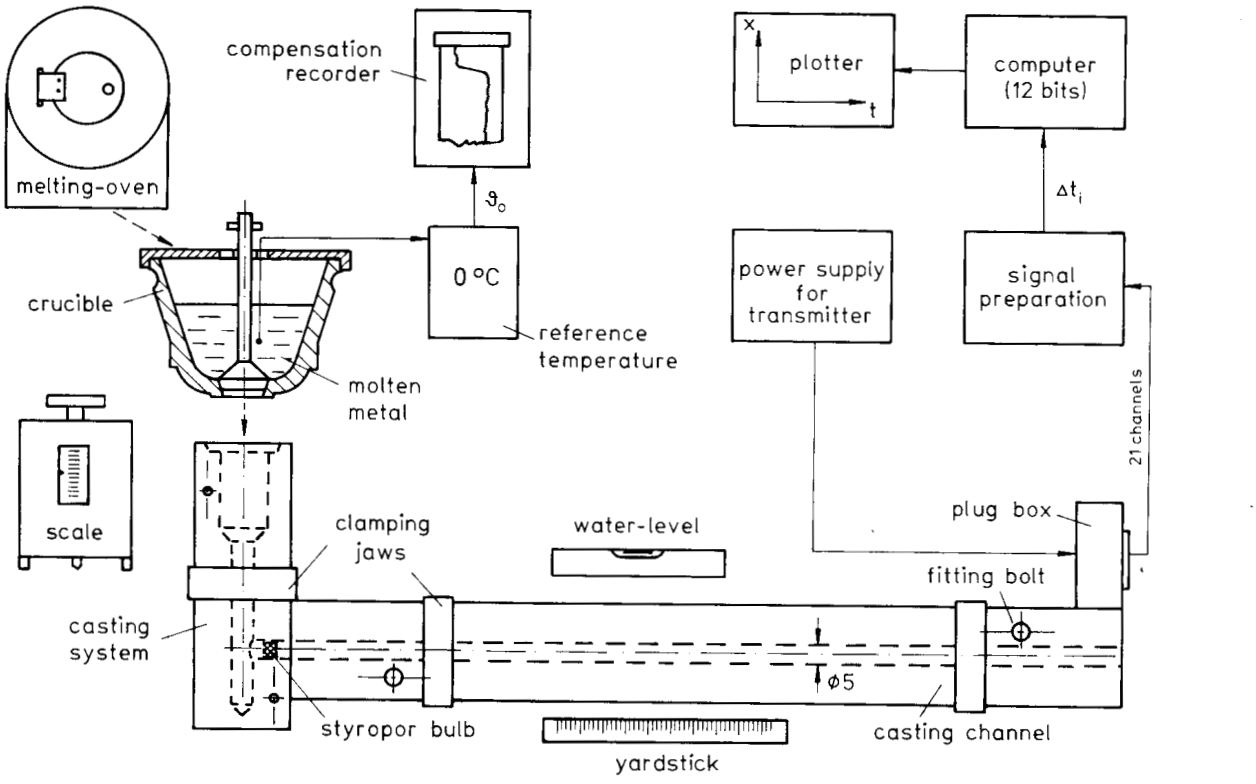


Fig.6. Schematic diagram of the experimental arrangement

3.2 Instrumentation

Unfortunately it is not possible to verify all the assumptions and theoretical results experimentally. For instance the development of the solidified annulus and the air-gap cannot be determined in the channel with established measurement techniques. But at least the progression of the flow-front shall be measured besides the values of casting temperature, wall temperature, metal head and fluidity.

The flow-function was already measured during fluidity testing by Czikel and Grossmann [3] and Morita [17]. They used insulated electrical contacts to track the flow-front. But they had difficulties with the melt, which did not always instantaneously close the electrical circuit. - Ragone et al. [20] used transparent glass tubes so that they could apply a fast movie camera (64 exp./s). But the tubes had to be destroyed after each test run. - For the own experiments also an optical measurement technique is applied using small photo cells along the channel. They are fixed into little horizontal holes ($\varnothing$ 2.4 mm) perpendicular to the channel axis with a transmitter (OP 124) and a receiver (OP 300) facing eachother. The components are designed for paper tape readers in computer industry (ESB [5], Ratheiser and Pichler [21]) and are here protected against thermal overload by transparent glass cylinders. The function of those photo cells and the electronic circuits for the signal preparation is explained by the block diagram in Fig.7.

As soon as the melt reaches the first photo cell and shades off the light from the transmitter (ca. 900 nm) the photo darlington transistor (OP 300) blocks and thus changes the voltage from a high level to a low level at the entrance of the mono-stable flip flop. The electronic switch is thereby turned on and holds the high output signal as long as the "reset" button is not pressed, regardless of any changes at the input. This signal is added to those of the other photo cells in a generator, referred to as parity generator (2k + 1), which changes the output level each time the number of input signals changes. Thus the continuous flow of the molten metal into the channel till its solidification is approximated by a rectangular function of time. The time intervals $\Delta t_i$ are

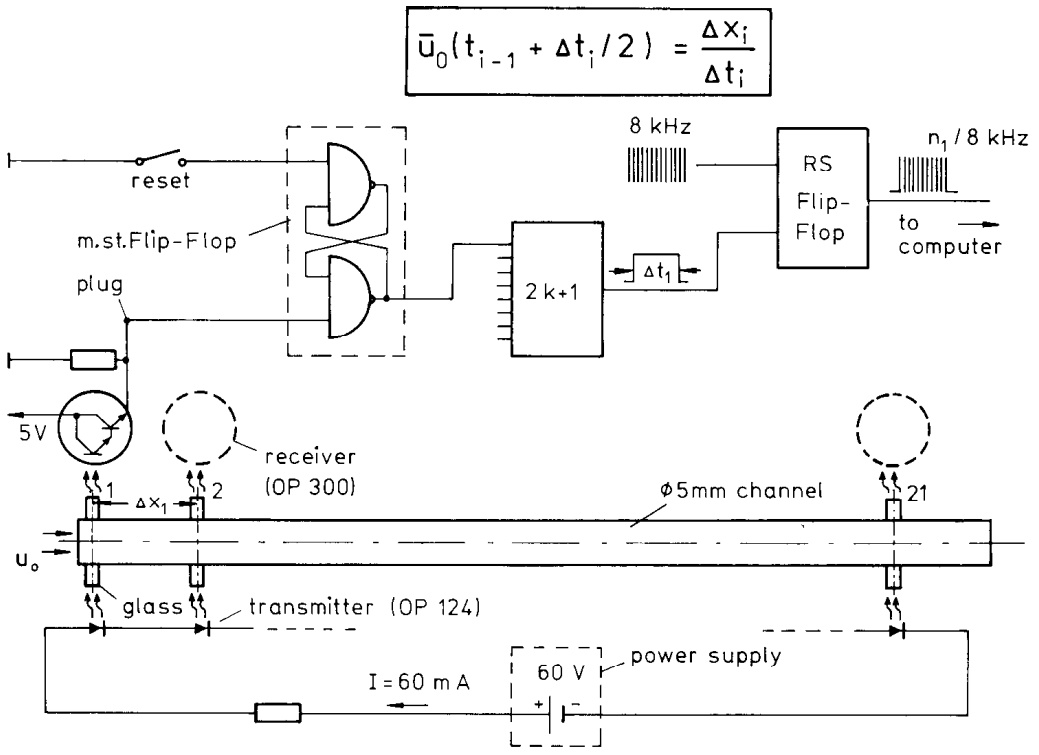


Fig.7. Block diagram of the optical measurement technique for flow function (flow-front velocity)

equivalent to the time which the melt needs to pass the distances $\Delta x_i$ between the 21 photo cells and are measured by comparison with a 8 kHz timer signal in the connected computer (Nova, Data General Corporation). When the flow stops the measurement is automatically concluded by exceeding the time limit of 0.512 s for one time interval (12 bits $\hat{=}$ 4096) and the results are plotted on a diagram (Fig.6). Thus the flow function can be obtained stepwise missing only the last time value when the total flow length (fluidity) is reached. The mean flow-front velocity can also be determined in a way demonstrated in Fig.7. - The average error of this measurement technique, considering the finite dimension of the photo cells and the time resolution limit of 1/8 ms, is usually less than 5 %.

The temperatures are measured with a sheathed NiCr-Ni thermoelement (Ø 1 mm) using an ice water reservoir (0 °C) as reference temperature. The analogous voltage is registered on a compensation recorder and transformed to temperatures using the calibration charts with a manufacturing tolerance of 0.75 %.

It was first tried to measure the casting temperature directly in front of the channel entrance by a very small thermocouple. But during the short test period (less than 1 s) an equilibrium value could not be obtained mainly because of local solidification. Therefore the casting temperature has always been measured in the crucible just before pouring into the casting system. Assuming that the melt does not cool significantly in the casting system of insulating material this value can be attributed to the initial condition for temperature $\vartheta_0$. - The fluidity and the metal head as further test quantities are measured with a yard-stick on the solidified and unmolded cast piece.

### 3.3 Test Procedure

To explain the course of an experiment on the whole the test procedure shall be described now (Fig.6). The metals are delivered from the manufacturer in granular form with a garanteed purity of more than 99.99 %. Random test analyses showed that even after casting under normal atmospheric conditions the cast pieces still contained less than 0.05 % impurities.

The metal is filled into the crucible and weighed on an electrical scale to adjust a certain metal head. Depending on metal density and metal head the mass usually ranges between 100 and 200 g. The crucible

is then put into a preheated melting oven where it is heated to the adjusted temperature (up to 1000 °C) in about one hour. In the meantime the two halfs of the channel form are carefully cleaned with acetone and fixed together. The halfs of the casting system with the introduced styropor bulb are clamped and screwed to the channel entrance. The channel is levelled horizontally with a water-level. The photo cells are connected to the box with the signal preparation through a 24-veined cable plugged to the plug box where the power supply for the transmitters also leads to. Finally all the instruments are switched on and the test program in the computer is started.

By means of specially constructed tongs with an opening device the crucible is taken out of the oven and put into the casting system. The sheathed thermocouple, which before served to measure the outer channel wall temperature, is dipped into the melt to determine the casting temperature registered on the compensation recorder. The plug is then drawn so that the melt flows into the casting system and after evaporizing the styropor bulb also into the horizontal channel. The oxide crust which covers the melt mostly remains in the crucible.

The test is finished then; the results of the optical flow measurement are automatically recorded and plotted. The fluidity as well as the metal head is determined from the cast piece after cooling and unmolding. - Some representative results shall be presented and compared with calculation in the following chapter.

## 4 Results and Discussion

### 4.1 Flow Function

The results of two experiments are shown in Fig.8.

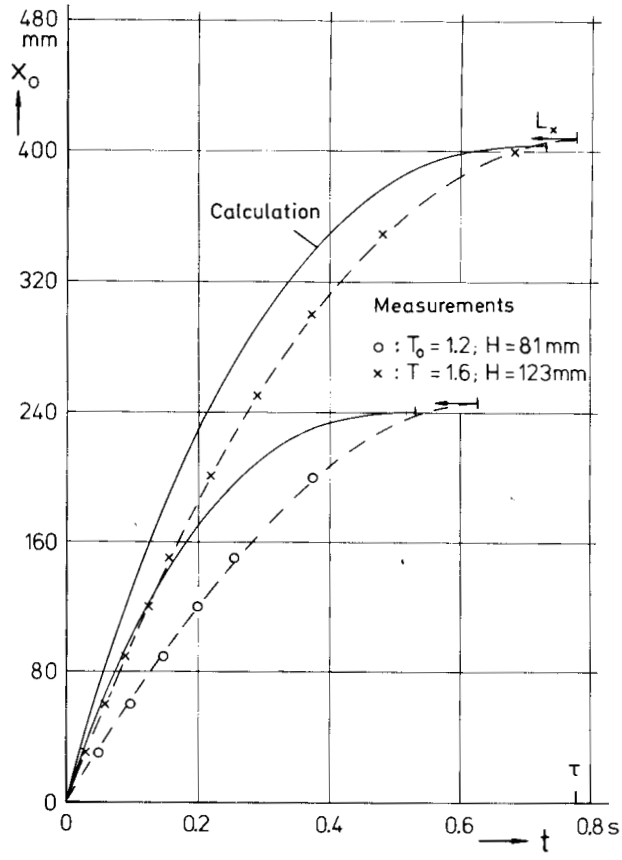


Fig.8. Two flow functions of tin for different casting conditions - comparison of calculation and measurement

For the different casting conditions also the calculated flow functions are demonstrated for comparison (for the applied property values see Table 1). It is obvious that the curvatures of the measured and calculated functions deviate considerably from each other. This means that the model predictions concerning the flow-front velocity do not correlate well with reality. But considering the rigorous simplification of quasi steady turbulent pipe flow one would not ex-

Table 1: Material properties as used in the calculations

| | | $\vartheta_s$ | $h_s$ | $\rho_l$ | $\rho_s$ | $c_l$ | $c_s$ | $\lambda_l$ | $\lambda_s$ | $a_s$ | $\nu$ | Pr | Ph ($\vartheta_u$ = 20° C) | $\lambda_a$ | $\beta$ |
|---|---|---|---|---|---|---|---|---|---|---|---|---|---|---|---|
| Tin | (Sn) | 232 | 59.4 | 6920 | 7130 | 248 | 255 | 32 | 60 | 33.0 | 0.28 | 0.014 | 1.09 | 0.04 | 0.027 |
| Lead | (Pb) | 327 | 23.4 | 10550 | 11400 | 160 | 150 | 15 | 31 | 18.1 | 0.204 | 0.025 | 0.50 | 0.045 | 0.035 |
| Zinc | (Zn) | 420 | 109 | 6600 | 6850 | 480 | 450 | 60 | 102 | 33.1 | 0.66 | 0.032 | 0.60 | 0.05 | 0.037 |
| Aluminium | (Al) | 660 | 396 | 2350 | 2550 | 1090 | 1200 | 92 | 212 | 69.3 | 0.47 | 0.013 | 0.51 | 0.06 | 0.034 |
| Inconel 600 | | 1400 | | | 8300 | | 520 | | 18 | 41.7 | | | | | |
| Grey Cast Iron | | | | | 6150 | | 710 | | 36 | 82.5 | | | | | |
| Molding Sand | | | | | 2150 | | 750 | | 1.3 | 0.81 | | | | | |
| Unit | | °C | $\frac{kJ}{kg}$ | | $\frac{kg}{m^3}$ | | $\frac{J}{kg \cdot K}$ | | $\frac{W}{m \cdot K}$ | $\frac{mm^2}{s}$ | $\frac{mm^2}{s}$ | — | — | $\frac{W}{m \cdot K}$ | $\frac{mm}{m \cdot K}$ |

peet much better consistency. To adjust the calculation to the experiments one could think of altering the friction coefficient or even the whole Blasius formula in Eq.(2); but since the reason for the deviations may also be a different solidification front, which we cannot check, we might just accept that we still know too little about such unsteady flows of solidifying fluids in order to describe it more accurately. Furthermore we are more interested in predicting fluidity and its dependence on various casting parameters than we are interested in each actual position of the flow-front. And as Fig.8 demonstrates the fluidity L turns out to be satisfactory as well as the total solidification time $\tau$, of which the experimental value has been extrapolated from the flow function. Thus these integral quantities prove that the overall energy balances are true. - In the next section we want to investigate whether this can be verified for the dependence of fluidity on different parameters, as well.

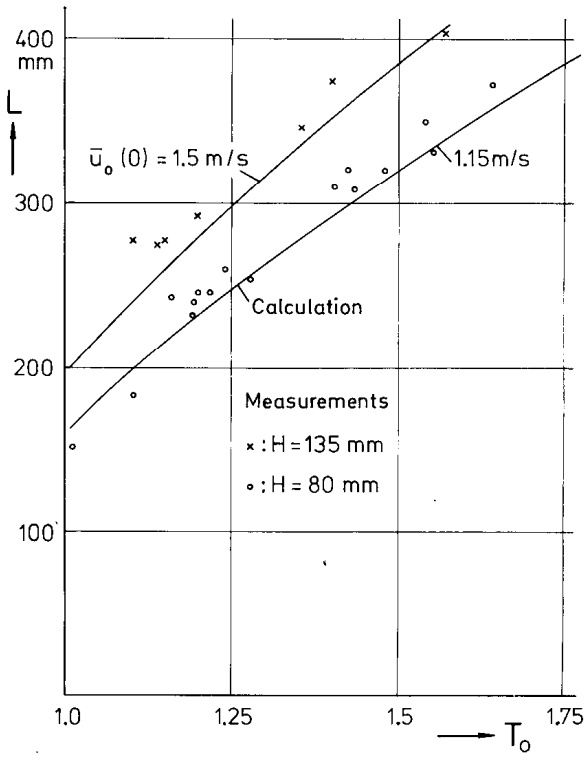


Fig.9. Fluidity of tin and its dependence on casting temperature and metal head (initial conditions) - comparison of calculation and measurement

## 4.2 Fluidity and its Dependence on Various Parameters

With the own experiments the effects of casting temperature and metal head can be investigated for different metals (material properties). The results of experiments with tin are collected in Fig.9, showing the dependence of fluidity on casting temperature for two different metal heads, i.e. initial flow-front velocities.

The measurements compare well with calculations; the scatter of the measurements might be due to variations in casting conditions (styropor bulb) and instrument errors. Considering also the uncertainties associated with property values and the simplifying assumptions the model predictions are quite satisfactory.

Most of the experiments have been conducted with tin since it can be handled most easily. However, to investigate the influence of material properties, also lead, zinc and aluminium have been cast. The agreement of measurement and calculation is not as good as for tin. Lead rather frequently shows cavities or dents along the flow length so that the channel cross section was not completely filled there, a phenomenon also observed by other authors (Klein and Fischer

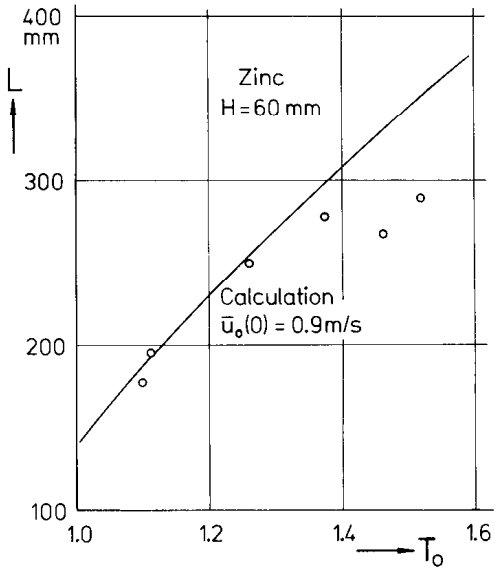


Fig.10. Influence of casting temperature on fluidity of zinc - comparison of calculation and measurement

[11]) but not being explained yet. - Zinc and aluminium have to be cast manually from a resistent crucible of graphite or ceramics because of their aggressive solubility towards other metals. In such a case the metal head might not be kept as constant as by the crucible shown in Fig.6. An example for these experiments is shown in Fig.10. Still, the influence of cast-

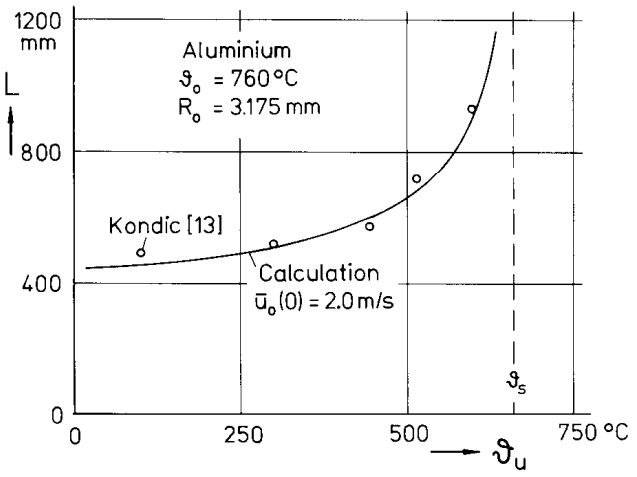


Fig. 11. Variation of fluidity with mold temperature in a grey cast iron spiral test form of Kondic and Kozlowski [13] - relative comparison of calculation and measurement

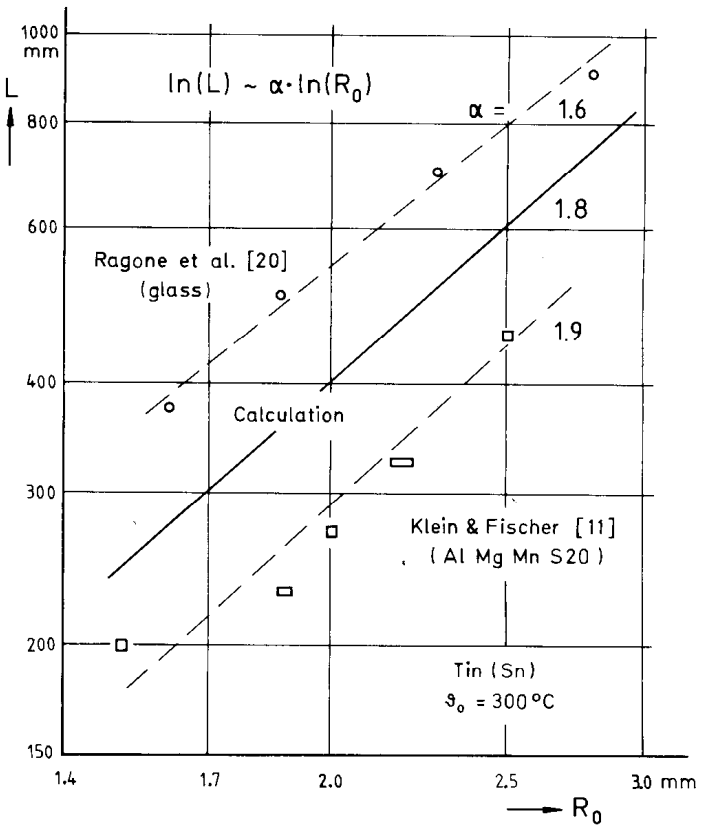


Fig. 12. Fluidity as function of channel radius (hydraulically equivalent) - relative comparison of calculation and measurement

ing temperature as well as the absolute value of fluidity is rather well predicted, thus proving that the dependence on property values is correctly described by the model.

The dependence on other parameters such as mold temperature has, for example, been investigated by Kondic and Kozlowski [13] in a spiral test form of grey cast iron which was electrically heated. The results are compared with calculation in Fig. 11. Since they give no indication of the exact metal head the initial value of $\bar{u}_0$ has been assumed, so that only the relative agreement of calculation and experiment can be stated here. Also the spiral form may have an effect on the absolute value of fluidity; but nevertheless the dependence on mold temperature is very well confirmed.

A last example for the experimental verification of the numerical results is given in Fig. 12. It shows the functional relation between fluidity and channel radius for different test forms. The measurements of Klein and Fischer [11] were performed in straight channels of aluminium alloy with different rectangular or square cross sections (see symbols). These values have been transformed to hydraulically equivalent radii and put into the double logarithmic diagram. The fitting lines then have a gradient of 1.6 and 1.9 for the measurements of Ragone et al. [20] in circular glass tubes (w = 0.6 ... 1.0 mm only) and Klein and Fischer [11] respectively. This agrees well with the calculated value of 1.8 independent of material properties.

### 4.3 A Theoretical Equation for Practical Use

After having verified the mathematical model experimentally it seems worth the effort to collect the numerical results, achieved by difficult and time-consuming computation, to a handy formula for fluidity. For this purpose, all important parameters relevant for the problem and contained in the governing equations of the model are gathered to a potential expression. Only the parameters representing solidification enthalpy and superheat are somewhat altered to a sum of exponentials, realizing that fluidity remains finite if either one of the parameters vanishes. Performing parameter analysis then on that expression one can determine the constants and exponents by fitting the numerical results. Thus the following equation is obtained:

$$\frac{L}{R_0} = 0.095 \cdot \left(\frac{\rho_s \cdot c_s}{\rho_w \cdot c_w}\right)^{0.14} \cdot \left(\frac{\rho_s \cdot c_s}{\rho_l \cdot \rho_l}\right)^{0.46} \cdot \left(\frac{\lambda_l}{\lambda_s}\right)^{0.8} \cdot$$

$$\cdot \left(\frac{\lambda_s}{\lambda_m}\right)^{0.52} \cdot Pr^{0.75} \cdot \overline{Re}(0)^{0.8} \cdot$$

$$\cdot [1 + 9 \cdot Ph^{0.8} + 19 \cdot (T_0 - 1)^{0.9}] \quad . \qquad (19)$$

The influence of the air-gap on fluidity is implied in the definition of $\lambda_m$ in Eq.(19). Similar to the formulation (15) for the thermal resistance between the neighboring grid points at the inner wall interface a mean value of the thermal conductivities of air and wall is defined:

$$\lambda_m \approx \left[\frac{\beta \cdot 0.1 \cdot (\vartheta_s - \vartheta_u)}{\lambda_a} + \frac{0.5}{\lambda_w}\right]^{-1} \quad . \qquad (20)$$

Since the actual temperature difference determining the air-gap width is not a priori known a fraction (20 %) of the maximum difference has been chosen by empirical evaluation.

Equation (19) represents the numerical results of the before described mathematical model within a maximum tolerance of 10 % for an application range of the parameters usually not exceeded in practice. Since those results have been experimentally verified Eq.(19) can be regarded as a formula for practical use requiring only the material properties and the casting parameters.

## 5 Concluding Remarks

The unsteady flow of pure metals into a horizontal cylinder has been analysed both theoretically and experimentally. The numerical results of a two dimensional mathematical model describing the problem of fluidity, a quantity defined by foundrymen, have been summarized to a theoretical equation by fitting analysis. It quantitatively describes the dependence of fluidity on the relevant parameters such as the material properties of metal and mold, the casting conditions (temperatures, metal head) and the channel radius. It does not contain any adjustable constants or empirical coefficients and thus is generally applicable to problems with similar initial- and boundary conditions.

It is, however, questionable whether the model is appropriate for the description of alloy casting, since alloys show a different mode of solidification with a temperature range for the phase change. But for an accurate verification the necessary property values have to be evaluated first, which are still hardly known even for pure metals concerning completeness and sufficient accuracy.

## Acknowledgement

This work has been supported by Deutsche Forschungsgemeinschaft (DFG) under Grant Nos. Gr 168/44-61.

## References

1. Beaubouef, R.T.; Chapman, A.J.: Freezing of Fluids in Forced Flow. Int. J. Heat Mass Transfer 10 (1967) 1581-1587
2. Bird, R.B.; Stewart, W.E.; Lightfoot, E.N.: Transport Phenomena. New York: John Wiley (1960)
3. Czikel, J.; Grossmann, H.: Zeitmessungen an einer stabförmigen Vergießbarkeitsprobe, deren wissenschaftliche und technische Auswertung. Freiberger Forsch. Heft B 8 (1955) 111-140
4. Epstein, M.; Yim, A.; Cheung, F.B.: Freezing-Controlled Penetration of a Saturated Liquid into a Cold Tube. J. Heat Transfer 99 (1977) 233-238
5. ESB-Gesamtkatalog: Elektronik-Bauteile und Meßgeräte. München (1976)
6. Flemings, M.C.: Solidification Processing. New York: McGraw-Hill (1974)
7. Genthner, K.: Das Erstarren und Schmelzen von reinen Stoffen und binären Gemischen bei turbulenter Strömung in Rohren. Dissertation, TU Berlin, Berlin (1972)
8. Goodrich, L.E.: Efficient Numerical Technique for One-Dimensional Thermal Problems with Phase Change. Int. J. Heat Mass Transfer 21 (1978) 615-621
9. Grigull, U.; Sandner, H.: Wärmeleitung. Springer, Berlin (1979)
10. Inconel Alloy 600: Publication 3269. England: H. Wiggin, Hereford, (1973)
11. Klein, F.; Fischer F.: Fließ- und Formfüllungseigenschaften metallischer Schmelzen. Metall 27 (1973) 326-335
12. Kölling, M.: Instationäre Wärmeübertragung mit Erstarrung am Beispiel des Fließvermögens reiner Metalle. Dissertation, TU München (1980)
13. Kondic, V.; Kozlowski, H.J.: Fundamental Characteristics of Casting Fluidity. J. Inst. Metals 75 (1949) 665-678
14. Krynitsky, A.I.: Progress Made in Fluidity Testing of Molten Metals During the Last Ten Years. Trans. Am. Fndrym. 61 (1953) 399-410
15. Lang, G.: Gießeigenschaften und Oberflächenspannung von Aluminium und binären Aluminiumlegierungen - Teil I: Fließvermögen. Aluminium 48 (1972) 664-672

16. Marsal, D.: Die numerische Lösung partieller Differentialgleichungen. Bibliographisches Institut. Zürich: (1976)
17. Morita, S.: Der Einfluß einer Unterkühlung auf das Fließvermögen geschmolzener Metalle. Gießerei-Beihefte 18 (1961) 109-122
18. Muehlbauer, J.C.; Sunderland, J.E.: Heat Conduction with Freezing or Melting. Appl. Mech. Rev. 18 (1965) 951-959
19. Myers, G.E.: Analytical Methods in Conduction Heat Transfer. New York: McGraw-Hill (1971)
20. Ragone, D.V.; Adams, C.M.; Taylor, H.F.: Some Factors Affecting Fluidity of Metals. Trans. Am. Fndrym. 64 (1956) 640-652
21. Ratheiser, L.; Pichler, H.: Optoelektronik. München: Franzis (1976)
22. Roache, P.J.: Computational Fluid Dynamics. Hermosa Publishers, Albuquerque, N.M. (1976)
23. Siegel, R.; Savino, J.M.: An Analysis of the Transient Solidification of a Flowing Warm Liquid on a Convectively Cooled Wall. Int. J. Heat Mass Transfer 12 (1969) 803-809
24. Smith, G.D.: Numerische Lösung von partiellen Differentialgleichungen. Braunschweig: Vieweg (1970)
25. Smithells, C.J.: Metals Reference Book, 4. ed. London: Butterworth (1967)
26. Sparrow, E.M.; Ramadhyani, S.; Patankar, S.V.: Effect of Subcooling on Cylindrical Melting. J. Heat Transfer 100 (1978) 395-402
27. Stefan, J.: Über die Theorie der Eisbildung, insbesondere über die Eisbildung im Polarmeer. Am. Phys. Chem. 42 (1891) 269-286
28. Stephan, K.: Influence of Heat Transfer on Melting and Solidification in Forced Flow. Int. J. Heat Mass Transfer 12 (1969) 199-213
29. Touloukian, Y.S.; Ho, C.Y.: Thermophysical Properties of Matter. TPRC-Data Series, IFI-Plenum Publ. Corp., New York (1970)
30. VDI-Handbuch Betriebstechnik: Physikalische Eigenschaften der reinen Metalle. VDI 3128. Berlin: Beuth (1977) p. 2

Dipl.-Ing. M. Kölling
Prof. Dr.-Ing. U. Grigull
Lehrstuhl A für Thermodynamik
Technische Universität München
Postfach 20 24 20
8000 München 2

Eingegangen am 8. Juli 1980